Received: 13 January 2022 | Revised: 20 March 2022 | Accepted: 23 March 2022
DOI: 10.1002/mmce.23172

ORIGINAL ARTICLE

INTERNATIONAL JOURNAL OF RF AND MICROWAVE COMPUTER-AIDED ENGINEERING WILEY

Conformal metal crack detection sensor based on flexible graphene film antenna

Cong Tong | **Rongguo Song** | **Huijuan Guan** | **Yingping Yang** | **Daping He**

Hubei Engineering Research Center of RF-Microwave Technology and Application, Wuhan University of Technology, Wuhan, China

Correspondence
Yingping Yang and Daping He, Hubei Engineering Research Center of RF-Microwave Technology and Application, Wuhan University of Technology, Wuhan 430070, China.
Email: ypyang@whut.edu.cn and hedaping@whut.edu.cn

Funding information
Fundamental Research Funds for the Central Universities, Grant/Award Numbers: 2020IB022, 205209016, 2020IB005; Wuhan Application Foundation Frontier Project, Grant/Award Number: 2020020601012220

Abstract
Crack detection of metal structures is an important procedure to ensure the safe operation of metal structures. In this work, a metal crack sensor based on a highly conductive flexible graphene film is proposed. The sensor is designed based on conformal microstrip antenna composed of a flexible graphene film radiation patch and a flexible dielectric substrate. The prepared sensor exhibited a detection sensitivity of 36.82 MHz/mm demonstrated by both experimental and simulation results. Moreover, benefiting from the flexible nature of the graphene film, the proposed sensor shows good conformality which makes up the shortcoming of the traditional rigid crack detection device.

KEYWORDS
conformal antenna, crack detection, flexible, graphene, sensor

1 | INTRODUCTION

In today's society, metal structures show wide-spread applications in aviation, automobiles, hoisting machinery, construction, and other fields. However, metal structures generally suffer inevitable fatigue cracks produced during long-term use which account for about 50%–90% of the failure of metal structures according to incomplete statistics.[1] In order to prevent serious accidents caused by cracks in the metal structure, the development of real-time monitoring technique of the formation of these cracks is crucial.

In recent years, many crack detection technologies have been developed. Eddy current, for example, is a commonly used method to detect cracks in metal structures as it does not require coupling or contact with the tested part and has high-detection sensitivity. However, eddy current testing is difficult to quantify cracks, and can only detect cracks near the surface which makes it difficult to detect some unreachable areas.[2,3] Also, the lift-off effect on the signal strength of eddy current monitoring also restricts the use of eddy current detection.[4,5] Ultrasonic signal detection, on the other hand, has the ability to detect the cracks deep beneath the surface. However, ultrasonic detection requires transmitting and receiving devices, and the signal processing process is complicated.[6,7] The optical fiber sensor is considered to be a very promising sensor, which has the advantages of high sensitivity and distributed arrangement but with prohibitive cost.[8–11] A spoof surface plasmon polaritons (SSPPs) sensor based on liquid switch control is proposed to detect metal surface cracks, the detection method is based on the change of reflection coefficient of SSPPs sensor caused by cracks.[12] However, the structure of this sensor is more complex, and the switch type should be used for control. In the meantime, microstrip antenna sensors not only have the advantages of small size, lightweight, low profile, and easy conformal,[13,14] but can also carry out real-time monitoring of the measured object in a portable way. In 2010, Mohammad and Huang

Cong Tong and Rongguo Song contributed equally to this work.

proposed crack detection based on microstrip antenna sensors and achieved a detection sensitivity of 22.1 MHz/mm.[15] In 2012, Mohammad reported the detection of crack direction using microstrip antenna sensor for the first time in which they utilized the two basic radiation patterns of TM_{01} and TM_{10} of the rectangular microstrip antenna to reflect the direction of the crack.[16] In 2017, Liu proposed a microstrip antenna sensor as crack detection in FRP-strengthened steel structure.[17] In 2018, Ke proposed a crack identification algorithm based on "crack flux," and verified that through experiments.[18] In the same year, Marindra proposed a chipless RFID sensor tag for metal crack detection and characterization.[19] In 2019, Dong designed a wireless passive sensor based on microstrip antenna for metal crack detection and characterization, but the sensor designed in this paper can only detect the width of the crack.[20] In the same year, Zhang proposed a configurable dielectric resonator based passive wireless sensor for crack monitorin.[21] In 2020, Xu designed an radio frequency identification (RFID) tag antenna to realize wireless detection of surface cracks on metal structures.[22] Although the above studies have proved that the microstrip antenna sensor can detect cracks in metal structures, the detected metal structures are mainly planar structures, and the monitoring sensitivity needs to be further improved. Traditional antenna sensors are usually made of metals such as copper and aluminum.[20–23] However, the metal structures have poor flexibility and are not easy to conform to curved structures,[24] which limit their applications in crack detection of curved metal structures. Even though it is mentioned in the reference that TE_{11} wave is used to detect cracks in curved metal structures.[25] However, this method cannot reflect the relevant information of cracks. In addition, antenna sensors based on metal structures have poor corrosion resistance, making it difficult to work stably for long time in harsh environments. At the same time, the rapid development of modern society requires antenna sensors to be lighter and more environmentally friendly. These problems greatly restrict the use of the microstrip antenna sensor based on metals.

Graphene, as the thinnest and lightest two-dimensional material composed of carbon atoms, has high electrical and thermal conductivity, as well as good flexibility.[26–29] In addition, as a carbon material, graphene has better chemical stability and adaptability to harsh environments than its metal counterparts.[30] Due to the excellent flexibility of graphene, it has been used in various wearable antennas such as pressure sensor,[31] ultra-wideband antenna,[32] near-field communication (NFC) tag antenna,[33] dual-band conformal antenna,[34] and millimeter wave antenna array,[35] which proves that graphene can be used in flexible devices.

In this article, a conformal microstrip antenna sensor based on flexible graphene film is proposed for crack detection suitable for curved metal structures. The radiation patch was processed by laser engraving with an overall antenna dimension of $25 \times 30 \times 0.027\ mm^3$. Combining the simulation and experimental results, the detection sensitivity was determined to be 36.82 MHz/mm on curved metal surface. Thus, the metal crack sensor based on flexible graphene films proposed in this article has important application value for the crack detection of metal structures, especially nonplanar metal structures.

2 | PRINCIPLE AND CONFIGURATION

2.1 | Graphene sensor design

The microstrip antenna consists of a three-layer structure, the upper radiation patch, the middle dielectric substrate, and the bottom metal ground plate. Considering the configuration of the patch antenna and the fact that any good conductor can be grounded. The graphene radiating patch (G-patch) and the flexible dielectric substrate are compounded together to form an antenna sensor use an adhesive to paste the antenna sensor onto the surface of the metal structure to be tested, as shown in Figure 1A. The graphene conformal microstrip antenna sensor includes a G-patch and a flexible dielectric substrate, and the metal structure used as a ground plate to form a conformal microstrip antenna. The graphene antenna sensor uses a microstrip antenna side-feed method to excite two radiation modes TM_{10} and TM_{01}, as shown in Figure 1B. Figure 1B shows the top view of the graphene metal crack sensor. In this article, polyethylene terephthalate (PET) is used as the flexible substrate. The thickness and dielectric constant of PET are 0.5 mm and 3.5, respectively. The loss tangent of PET is 0.01. The flexible graphene sensor is attached to a metal aluminum cylinder with radius of 50 mm. The specific dimensions of the graphene sensor are given in Table 1.

In this case, the metal structure acts as a metal ground plate, and the formed conformal patch antenna sensor can sense certain physical changes of the metal structure. There are three directions of cracks on the metal grounding plate, along the width direction (W-crack), length direction (L-crack) and inclination direction (I-crack) of G-patch. It should be noted that the inclination angle of the I-crack in the simulation and experiment is 45 degrees. For example, when no crack appears on the metal structure (Figure 1C) to be tested. The currents of the two basic radiation modes of the conformal microstrip antenna will be along the length and width of the metal ground plate respectively. When crack

INTERNATIONAL JOURNAL OF RF AND MICROWAVE COMPUTER-AIDED ENGINEERING WILEY

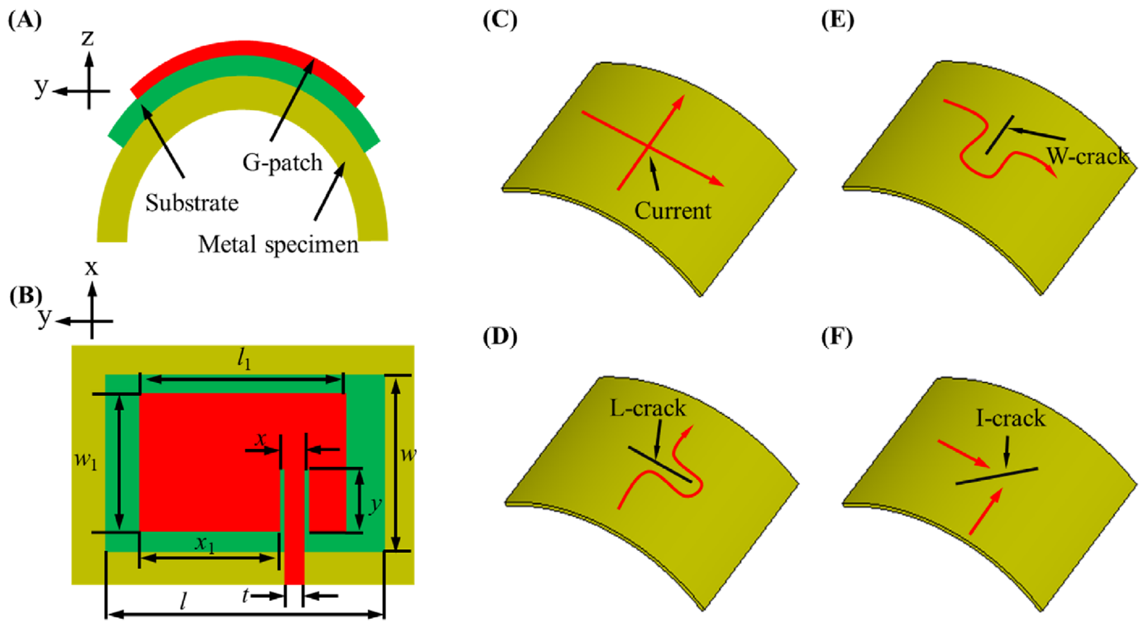

FIGURE 1 (A) Side view of schematic illustration of graphene cylindrical conformal microstrip antenna sensor structure, (B) top view of schematic illustration of graphene cylindrical conformal microstrip antenna sensor structure, (C) current flow without crack, (D) effect of W-crack on current flow, (E) effect of L-crack on current flow, (F) effect of I-crack on current flow

TABLE 1 Detailed parameters of the designed graphene sensor

Parameter	Values (mm)	Parameter	Values (mm)
w_1	25.00	l_1	30.00
w	50.00	l	60.00
x	2.25	y	8.00
x_1	17.87	t	1.25

appears on the metal structure to be tested, it will affect the current path on the ground plate of the conformal antenna as shown in Figure 1D–F. The current path becomes longer due to the occurrence of cracks, and cracks in different directions have different effects on the two basic mode currents. According to transmission line theory,[36] the resonant frequency of the antenna sensor is:

$$f_{mn} = \frac{c}{2\sqrt{\varepsilon_{re}}}\left[\left(\frac{m}{l}\right)^2 + \left(\frac{n}{w}\right)^2\right]^{1/2}. \tag{1}$$

$$f_{mn}(\text{crack}) = \frac{c}{2\sqrt{\varepsilon_{re}}}\left[\left(\frac{m}{l+\Delta l_{crack}}\right)^2 + \left(\frac{n}{w+\Delta w_{crack}}\right)^2\right]^{1/2}. \tag{2}$$

In Equations (1) and (2), c is the speed of light, ε_{re} is the equivalent dielectric constant of the dielectric substrate, l and w are the length of the corresponding mode current and m and n are the pattern numbers of the antenna. Δl_{crack} and Δw_{crack} are the increment of the current path caused by the crack It can be seen from Equation (1) Equation (2), when cracks appear, the resonant frequency of the antenna will decrease.

2.2 | Graphene sensor simulation

In order to verify the ability of the graphene sensor to detect cracks in curved metal structures, electromagnetic simulations were carried out using CST STUDIO SUITE software. Cracks with width of 1 mm and varying lengths of 0, 4, 8, 12, 16, and 20 mm were designed on the grounding plate. For each dimension of the crack, three possible orientations were taken into account, I-crack inclined at 45 degrees. As shown in Figure 2A, for the L-crack, as the crack expands, the resonant frequency f_{01} of the crack sensor along the x direction mode TM_{01} continued to decrease, while the resonant frequency f_{10} of the TM_{10} mode along the y direction was not affected. For the W-crack, as the crack expands, the resonant frequency f_{10} of the TM_{10} mode along the y direction continued to decrease, while the resonant frequency f_{01} of the TM_{10} mode along the x direction showed negligible change as shown in Figure 2B. In addition, for the crack formed along the off-diagonal direction, the resonance frequencies in both directions were affected to some extent (Figure 2C). It should be noted that the different length of the crack leads to the different impedance of

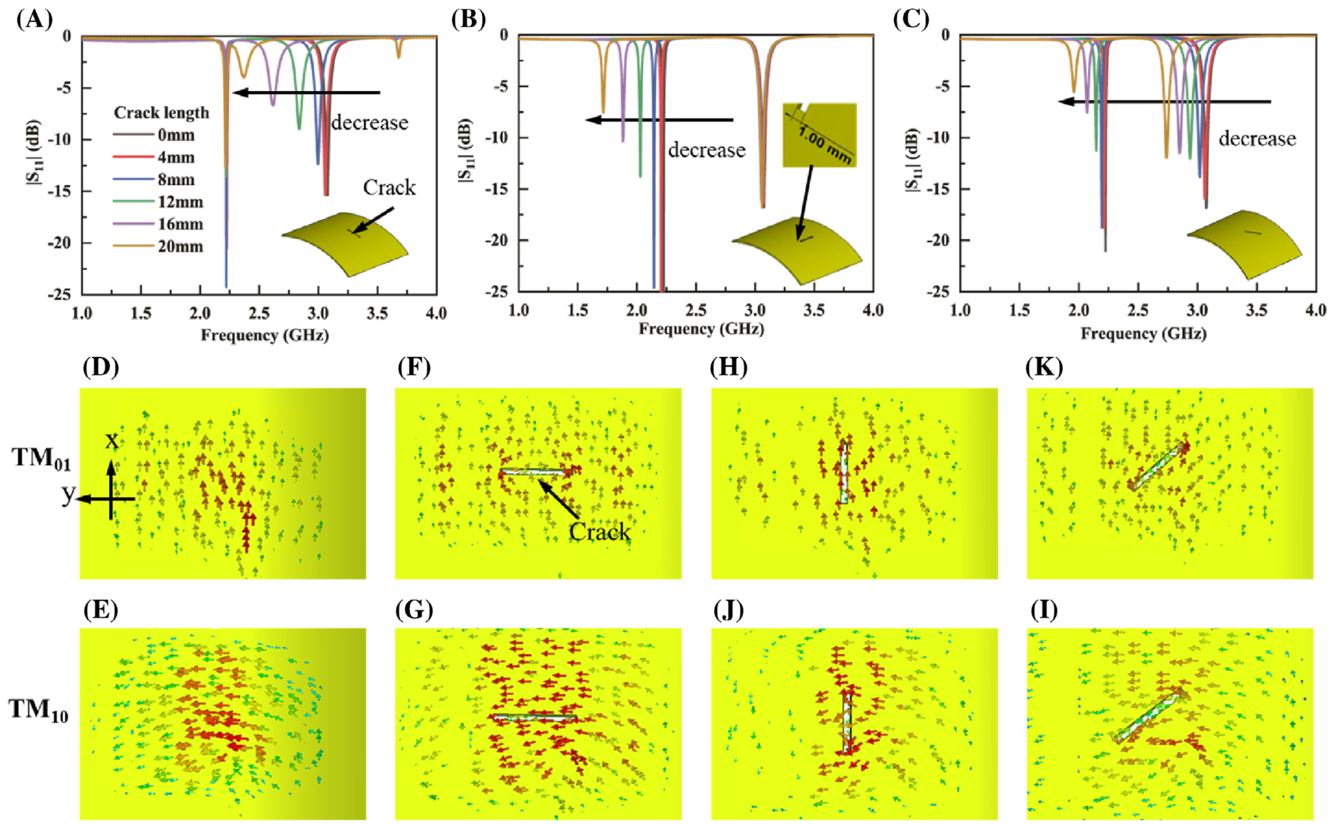

FIGURE 2 Simulated results: (A) the frequency response of graphene sensor to L-crack, (B) the frequency response of graphene sensor to W-crack, (C) the frequency response of graphene sensor to I-crack, (D) current distribution of TM_{01} mode on ground plate without crack, (E) current distribution of TM_{10} mode on ground plate without crack, (F) current distribution of TM_{01} mode on ground plate with L-crack, (G) current distribution of TM_{10} mode on ground plate with L-crack, (H) current distribution of TM_{01} mode on ground plate with W-crack, (I) current distribution of TM_{10} mode on ground plate with W-crack, (J) current distribution of TM_{01} mode on ground plate with I-crack, (K) current distribution of TM_{10} mode on ground plate with I-crack

antenna sensor. When there is no crack, the input impedance of the antenna sensor can be well matched with the characteristic impedance of the feeding microstrip line. With the expansion of the crack, the impedance mismatch between the antenna sensor and the feeding microstrip line becomes more and more serious, resulting in the decrease of $|S_{11}|$ depth at the resonant frequency.

Next, the influence of crack on resonant frequency is analyzed from the perspective of current. The current distribution of the ground plate of the graphene conformal microstrip antenna sensor is shown in Figure 2D–K. From Figure 2D,E, it can be seen that when there is no crack on the curved metal grounding plate, the current distributions of the TM_{01} mode and TM_{10} mode are along the x and y directions respectively. When cracks formed along the y direction on the curved metal grounding plate, the original TM_{01} mode current flow in the W direction changed, causing the TM_{01} mode current to flow around the crack, thereby increasing the effective electrical length of the antenna as shown in Figure 2F. From Equation (1), it can be seen that the resonant frequency of the antenna TM_{01} mode will decrease. Figure 2G shows that the crack along the y direction has little effect on current distribution of the TM_{10} mode along the y direction, so its influence on the resonant frequency of the antenna's TM_{10} mode is also very small. Similarly, from Figure 2H,I, it can be seen that the crack along the x direction changes the current distribution of the antenna's TM_{10} mode, but has little effect on the TM_{01} mode. Also, for the crack oriented off-diagonally with both x and y components, the current distribution of both the TM_{10} and TM_{01} modes are affected (Figure 2J,K).

So when a crack forms on the metal structure, it will affect the current distribution on the metal ground plate. Depending on the direction of the mode, the two modes for TM_{01} and TM_{10} will be affected differently and the current mode affected by different crack directions is different, which will shift resonant frequency of different antenna modes. Therefore, the length and direction of the crack on the metal ground plate can be reflected by measuring the change of the TM_{10} and TM_{01} resonant frequencies of the conformal microstrip antenna.

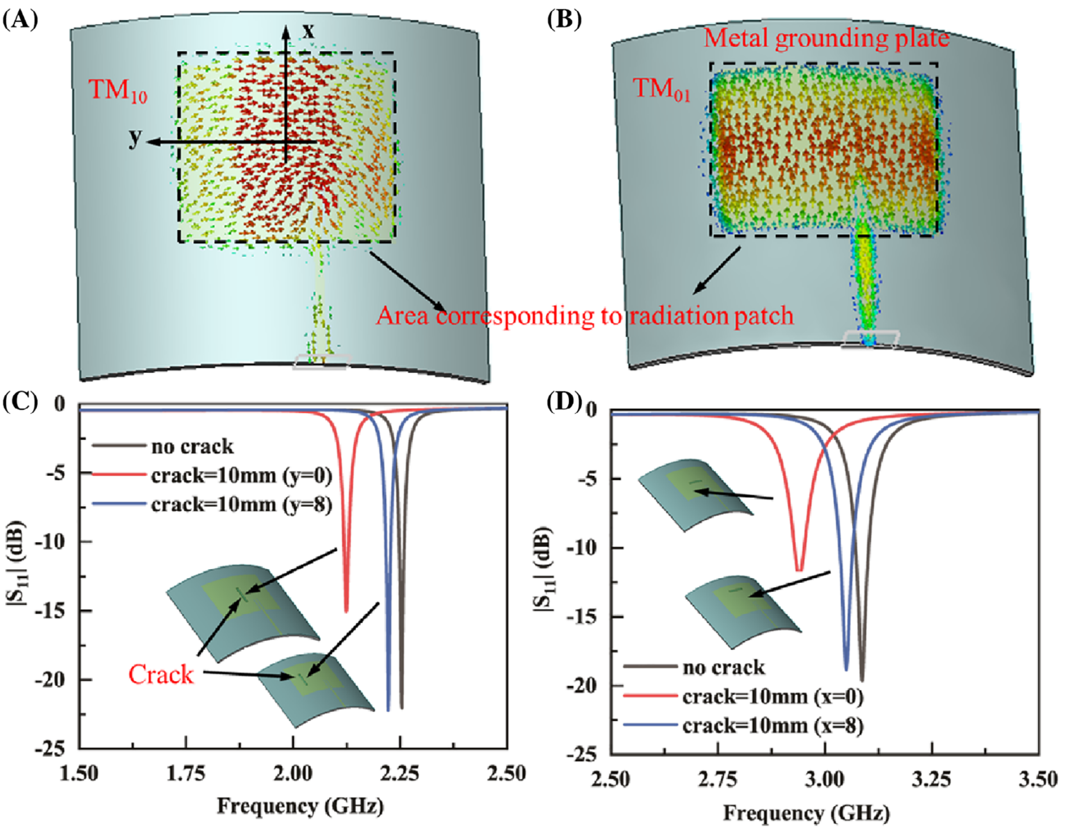

FIGURE 3 (A) Current distribution of TM_{10} mode on metal grounding plate, (B) current distribution of TM_{01} mode on metal grounding plate, (C) the influence of different positions of cracks on the y-axis on the resonant frequency of the sensor, (D) the influence of different positions of cracks on the x-axis on the resonant frequency of the sensor

2.3 | Crack location and angle

It should be noted that in the above simulation and subsequent experiments, the crack occurs in the middle of the corresponding area of the metal grounding plate radiation patch. The influence of different positions of cracks on the ground plate on the resonant frequency of the sensor is different (as shown in Figure 3). As shown in Figure 3A,B, We can see that the current distribution of TM_{10} mode or TM_{01} mode on the metal grounding plate is limited to the area corresponding to radiation patch and there is no current distribution at other locations of the metal grounding plate. So cracks can be detected only when they appear in the corresponding area of the radiation patch on the ground plate. At the same time, it can be found that the current distribution of TM_{10} mode and TM_{01} mode is uneven. The current in the middle of the distribution area is large and the current at the edge is small. So the crack appears in the middle of the mode current distribution region, which has a greater influence on the resonant frequency of the sensor than the edge as shown in Figure 3C,D.

Figure 4 shows the influence of the same crack on the resonant frequency of the sensor at different angles.

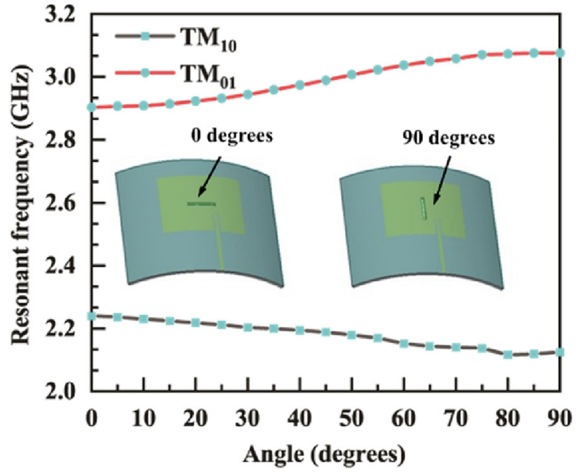

FIGURE 4 Effect of crack angle on resonant frequency

When the crack changes from 0 to 90 degrees, the resonant frequency of TM_{01} mode will continue to rise, which shows that the influence of crack on TM_{01} mode becomes little, while the resonant frequency of TM_{10} mode will continue to decline, and the influence of crack on TM_{10} mode becomes great. The angle information of crack can

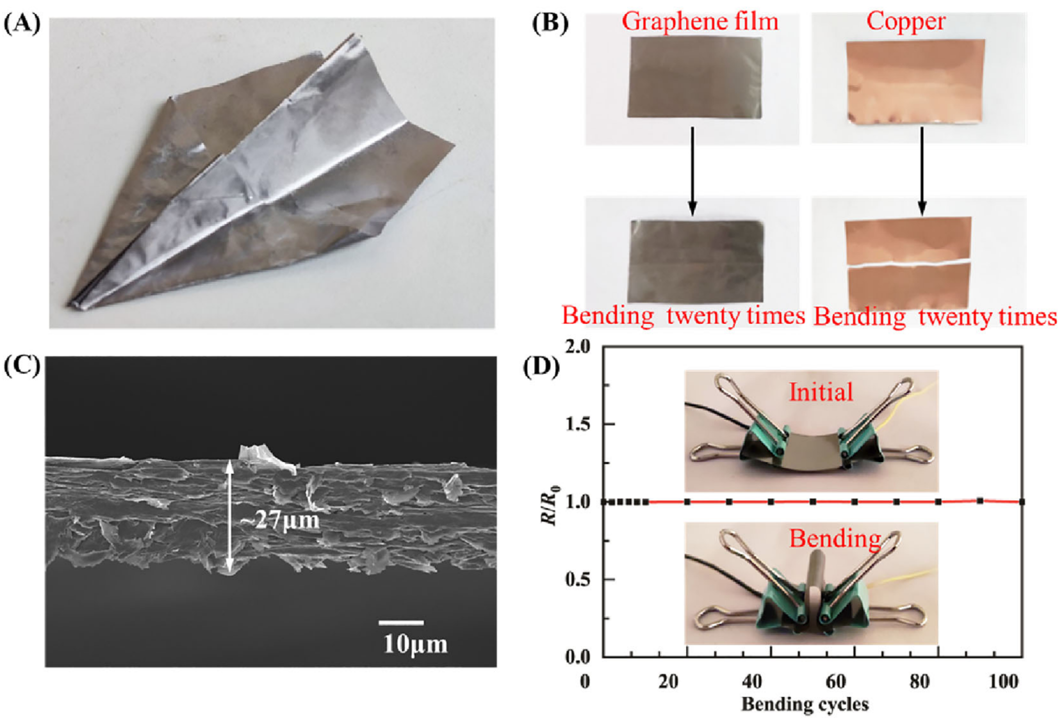

FIGURE 5 (A) A model airplane made of graphene film, (B) graphene film and copper foil folded test, (C) cross-sectional scanning electron microscope (SEM) image of graphene film, (D) the flexibility and mechanical stability test of graphene assembled films

be reflected by the change of resonant frequency of sensor TM_{01} mode and TM_{10} mode.

3 | FABRICATION AND MEASUREMENT

3.1 | Graphene assemble film

Figure 5A shows an airplane model made of graphene film, demonstrating excellent flexibility of the graphene film. It can be seen from the cross-sectional scanning electron microscope (SEM) image (Figure 5C) that the thickness of the flexible graphene film is ~27 μm. At the same time, the cross-sectional view also shows that the graphene film is a layered structure composed of graphene nanosheets, which provides good flexibility for the graphene film. To further verify the flexibility and mechanical stability of the flexible graphene film, a bending test is carried out as shown in Figure 5D. The relative resistance of the graphene film shows a constant value, which show that graphene film has good mechanical stability and flexibility. In Figure 5B, the surface of the graphene film is still very flat after 20 times of folding in half. However, the copper foil has broken after being folded in half for 20 times.

3.2 | Processing and testing of graphene sensor

The manufacturing process of the graphene antenna sensor is shown in Figure 6A. The fabrication of graphene radiation patch was achieved by the laser engraving machine to remove the unwanted parts and then compressed with the PET substrate to form graphene sensor which is shown in Figure 6B. Finally, the prepared graphene sensor was conformed to the metal structure to be tested. The test environment of the graphene sensor is shown in Figure 6C. The graphene sensor is connected to a vector network analyzer (VNA) through a coaxial cable to test its frequency response curve. In order to detect the crack growth, a metal aluminum cylinder with $R = 50$ mm and a thickness of 1 mm was loaded with metal cracks with a width of 1 mm and a length of 4, 8, 12, 16, and 20 mm. There are three directions of cracks, W-crack, L-crack, and I-crack. The metal structures and cracks were processed by a metalworking company (Shenzhen Dezheng hardware mold Co., Ltd). The cracks are produced by laser cut according to the dimensions we provide. The material of the metal structure is aluminum.

The resonant frequencies of the graphene sensor with different crack lengths and directions are shown in Figure 7A–C. The resonant frequency of the graphene sensor decreased as the crack length increased. As shown

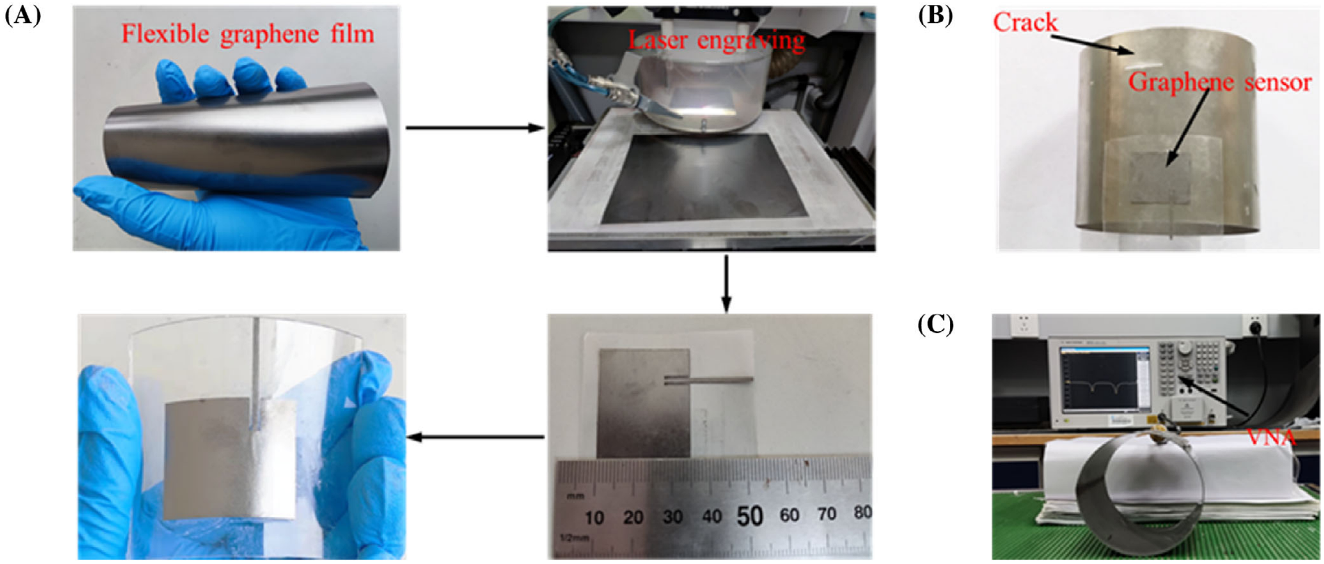

FIGURE 6 (A) Fabrication procedures of graphene conformal metal crack sensor, (B) graphene metal crack sensor, (C) measurement of graphene metal crack sensor

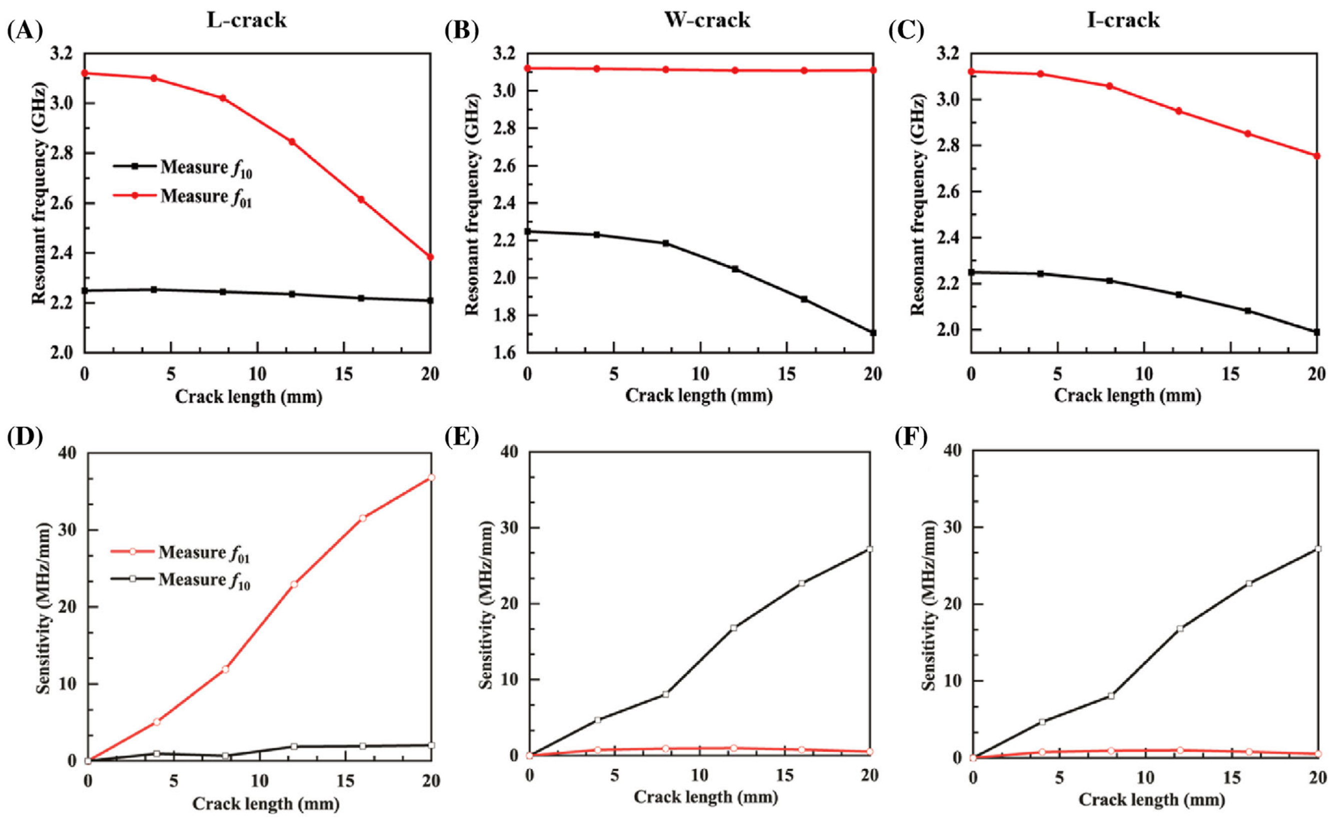

FIGURE 7 Measure result (A–C) the resonant frequency response to cracks oriented along (A) the y direction, (B) the x direction, and (C) the off-diagonal direction. (D–F) Detection sensitivity of graphene metal crack sensor to cracks oriented along (D) the y direction, (E) the x direction, and (F) the off-diagonal direction

in Figure 7A,B, cracks along the y direction and along the x direction caused the resonant frequency of the TM_{01} mode and the resonant frequency of the TM_{10} mode to decrease, respectively, and there was almost no effect on the other mode. In Figure 7C, the formation of an off-diagonal crack with an inclination angle of 45 degrees caused the resonant frequencies of the TM_{10} and TM_{01} modes to decrease simultaneously.

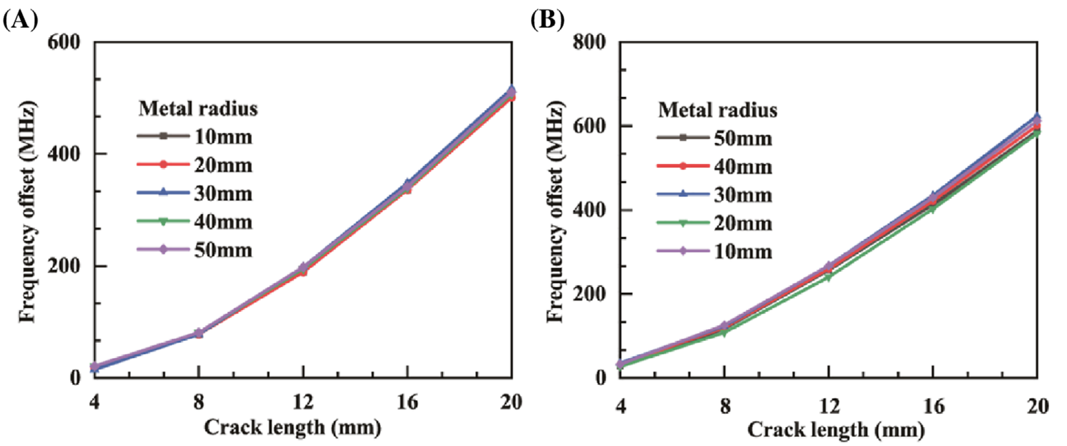

FIGURE 8 Frequency offset response of graphene sensor to different metal cylinder radii: (A) TM_{10} mode, (B) TM_{01} mode

TABLE 2 Properties comparison of crack sensors in this work and references

Reference	Size (mm)	Material	Sensitivity (MHz/mm)	Layers	Metal structures
21	$\pi \times 12 \times 12 \times 9$	Ceramic	25.4	1	Flat structure
19	$35 \times 15 \times 0.035$	Copper	153	2	Flat structure
15	$15.24 \times 12.7 \times 0.065$	Copper	22.10	2	Flat structure
17	$40 \times 28 \times 0.05$	Copper	29.37	3	Flat structure
18	$40 \times 28 \times 0.05$	Copper	33.50	2	Flat structure
20	22×20	silver	45.00	2	Flat structure
This work	$30 \times 25 \times 0.027$	Graphene film	36.82	2	Curved structure

Figure 7D–F shows the detection sensitivity of graphene metal crack sensor to cracks oriented along the y direction, the x direction and the off-diagonal direction respectively. In formula (3), f_r is the resonant frequency of the sensor itself when there is no crack and f_l is the resonant frequency of the sensor when the crack length is l. It can be found that when the crack just starts to expand, the sensitivity of crack detection is low at about 11.90 MHz/mm. As the crack expands more, the crack detection becomes more sensitive. Finally, the sensitivity of sensor is about 36.82 MHz/mm. From Figure 7D,E, we can see the sensitivity of L-crack is larger than the sensitivity of W-crack because of the length and width of graphene radiation patch are different. This is because the antenna size corresponding to the resonant frequency f_{01} is smaller, and the smaller the size of the sensor, the higher the sensitivity of detecting cracks

The detection effect of the sensor for cracks with different curvature can be seen from Figure 8 that as the crack length increases, the resonant frequency offset of the graphene sensor will continue to rise, and the crack loading on the metal ground plate with different curvatures will affect the resonant frequency of the graphene conformal microstrip antenna sensor is similar, which proves that the graphene conformal crack sensor has a good detection effect for metal structures with different curvatures.

$$Sensitivity = \frac{|f_l - f_r|}{l}. \quad (3)$$

Table 2 provides the properties comparison between the crack sensors in this work and references. Compared with other methods in references, the crack sensor proposed in this paper adopts flexible graphene film to realize conformal design with nonplanar structure, which greatly expands the application range of the sensor. In addition, the sensitivity of GAF sensor is 36.82 MHz/mm. Although the sensitivity mentioned in document 2 is very high, the sensor structure in document 2 is complex, two horn antennas are needed for detection, and the data processing is also complex.

4 | CONCLUSIONS

In conclusion, a metal crack sensor based on a flexible graphene film is proposed in this article. The graphene sensor has excellent detection capabilities for cracks formed in curved metal structures. It can not only detect the existence of cracks, but also detect the length and direction of the cracks. The detection sensitivity is 36.82 MHz/mm. Therefore, the graphene sensor has important application value for the crack detection of metal structures, especially for nonplanar metal structures.

ACKNOWLEDGMENT

This work was supported by the Wuhan Application Foundation Frontier Project (Grant No. 2020020601012220) and the Fundamental Research Funds for the Central Universities (WUT: 2020IB022, 205209016, and 2020IB005). Graphene film is provided by Wuhan Hanxi Technology Co., Ltd.

DATA AVAILABILITY STATEMENT

The data that support the findings of this study are openly available in Hubei Engineering Research Center of RF-Microwave Technology at http://wlsys.whut.edu.cn/work/index.html.

ORCID

Daping He https://orcid.org/0000-0002-0284-4990

REFERENCES

1. Foong CH, Wiercigroch M, Deans WF. Novel dynamic fatigue-testing device: design and measurements. *Meas Sci Technol*. 2016;17(8):2218-2226.
2. Liang C, Tian GY. Surface crack detection for carbon fiber reinforced plastic (CFRP) materials using pulsed Eddy current thermography. *IEEE Sens J*. 2011;11(12):3261-3268.
3. Adewale ID, Tian GY. Decoupling the influence of permeability and conductivity in pulsed Eddy-current measurements. *IEEE Trans Magn*. 2013;49(3):1119-1127.
4. Abidin IZ, Mandache C, Tian GY, Morozov M. Pulsed eddy current testing with variable duty cycle on rivet joints. *NDT & E Int*. 2009;42(7):599-605.
5. He Y, Luo F, Pan M, et al. Pulsed eddy current technique for defect detection in aircraft riveted structures. *NDT & E Int*. 2010;43(2):176-181.
6. Volkovas V, Dulevicius J. Acoustic emission used for detection of crack generation in propellers of turbine-pump units. *Russian J Nondestr Test*. 2006;42(4):248-254.
7. Sedlak P, Sikula J, Lokajicek T, Mori Y. Acoustic and electromagnetic emission as a tool for crack localization. *Meas Sci Technol*. 2008;19(4):045701.
8. Kang HK, Bang HJ, Hong CS, Kim CG. Simultaneous measurement of strain, temperature and vibration frequency using a fibre optic sensor. *Meas Sci Technol*. 2002;13(8):1191-1196.
9. Lee B. Review of the present status of optical fiber sensors. *Optical Fiber Technl*. 2003;9(2):57-79.
10. Sekine H, Fujimoto SE, Okabe T, Takeda N, Yokobori T. Structural health monitoring of cracked aircraft panels repaired with bonded patches using fiber bragg grating sensors. *Appl Compos Mater*. 2009;89(2):224-234.
11. Rodrigo A, Silva-Muñoz RA. Structural health monitoring of marine composite structural joints using embedded fiber Bragg grating strain sensors. *Compos Struct*. 2006;13(2):87-98.
12. Su PQ, Yang XQ, Wang J, Wang ZD, Peng HJ. Detection of metal surface cracks based on liquid switch controlled spoof surface plasmon polaritons. *IEEE Sens J*. 2022;22(2):1287-1294.
13. Varamini G, Keshtkar A, Naser-Moghadasi M. Compact and miniaturized microstrip antenna based on fractal and metamaterial loads with reconfigurable qualification. *AEU: Archiv Fur Elektronik Und Ubertragungstechnik: Electron Commun*. 2018;83:213-221.
14. Honarbakhsh B. High-gain low-cost microstrip antennas and arrays based on FR4 epoxy. *AEU-Int J Electron C*. 2017;75:1-7.
15. Mohammad I, Huang H. Monitoring fatigue crack growth and opening using antenna sensors. *Smart Mater Struct*. 2010;19(5):055023.
16. Mohammad I, Gowda V, Zhai H, Huang H. Detecting crack orientation using antenna sensors. *Meas Sci Technol*. 2012;7981(8):765-768.
17. Liu ZP, Chen K, Li ZC, Jiang X. Crack monitoring method for an FRP-strengthened steel structure based on an antenna sensor. *Sensor*. 2017;17(10):2394.
18. Ke L, Liu Z, Yu H. Characterization of a patch antenna sensor's resonant frequency response in identifying the notch-shaped cracks on metal structure. *Sensors*. 2018;19(1):1-18.
19. Marindra A, Tian GY. Chipless RFID sensor tag for metal crack detection and characterization[J]. *IEEE Trans Microwave Theory Techn*. 2018;66(5):2452-2462.
20. Dong H, Kang W, Liu L, Wei K, Xiong J, Tan Q. Wireless passive sensor based on microstrip antenna for metal crack detection and characterization[J]. *Meas Sci Technol*. 2019;30(4):1-14.
21. Zhang J, Huang H, Huang C, et al. A configurable dielectric resonator-based passive wireless sensor for crack monitoring [J]. *IEEE Trans Antennas Propag*. 2019;67(8):5746-5749.
22. Xu YW, Dong LH, Wang HD, Xie XZ, Wang P. Surface crack detection and monitoring in metal structure using RFID tag. *Sens Rev*. 2020;40(1):81-88.
23. Marindra AMJ, Tian GY. Chipless RFID sensor tag for metal crack detection and characterization. *IEEE Trans Microwave Theory Techn*. 2018;66:1-11.
24. Inui T, Koga H, Nogi M, Komoda N, Suganuma K. A miniaturized flexible antenna printed on a high dielectric constant Nanopaper composite. *Adv Mater*. 2020;27(6):1112-1116.
25. Chen GR, Katagiri T, Yusa N, Hashizume H. Experimental investigation on bend-region crack detection using TE11 mode microwaves. *Nondestr Test Eval*. 2021;37(1):71-80.
26. Wang J, Guan Y, Yu H, et al. Transparent graphene microstrip filters for wireless communications. *J Phys D Appl Phys*. 2017;50(34):34LT01.
27. Maosheng C, Xixi W, Min Z, et al. Electromagnetic response and energy conversion for functions and devices in low-dimensional materials. *Adv Funct Mater*. 2019;29(25):1807398.1-1807398.54.
28. Yao Y, Cheng X, Qu SW, Yu J, Chen X. Graphene-metal based tunable band-pass filters in the terahertz band. *IET Microwave Antennas Propag*. 2016;10(14):1570-1575.
29. Song R, Wang Z, Zu H, et al. Wideband and low sidelobe graphene antenna array for 5G applications[J]. *Sci Bull*. 2021;66(2):103-106.
30. Zhang N, Wang Z, Song R, et al. Flexible and transparent graphene/silver-nanowires composite film for high electromagnetic

interference shielding effectiveness. *Sci Bull*. 2019;64(8): 540-546.
31. Tang D, Wang Q, Wang Z, et al. Highly sensitive wearable sensor based on a flexible multi-layer graphene film antenna. *Sci Bull*. 2018;63(9):574-579.
32. Fang R, Song R, Zhao X, Wang Z, Qian W, He DP. Compact and low-profile UWB antenna based on graphene-assembled films for wearable applications. *Sensors*. 2020;20(9):2552.
33. Li S, Song R, Zhang B, Huang BQ, Zhao X, He DP. Wearable near-field communication bracelet based on highly conductive graphene-assembled films. *Int J RF Microwave Comput-Aided Eng*. 2021;31(1):22479.
34. Hu ZL, Xiao Z, S J, Song R, D H. A dual-band conformal antenna based on highly conductive graphene-assembled films for 5G WLAN applications. *Materials*. 2021;14(17):5087.
35. Song R, Zhao X, Wang Z, et al. Sandwiched graphene clad laminate: a Binde-free flexible printed circuit board for 5G antenna application[J]. *Adv Eng Mater*. 2020;22(10):2000451.
36. Carver K, Mink J. Microstrip antenna technology. *IEEE Trans Antennas Propag*. 2003;29(1):2-24.

How to cite this article: Tong C, Song R, Guan H, Yang Y, He D. Conformal metal crack detection sensor based on flexible graphene film antenna. *Int J RF Microw Comput Aided Eng*. 2022; e23172. doi:10.1002/mmce.23172